

SUPERCONDUCTIVITY AND STRUCTURE IN
 $\text{La}_{2-x}\text{M}_x\text{CuO}_4$, M=Ba, Sr, AND (Nd,Sr)

Arnold R. Moodenbaugh
Brookhaven National Laboratory
Upton, NY 11973-5000
moodenba@bnl.gov

Book Chapter Submitted to:

In Studies of High Temperature Superconductors: Advances in Research and Applications, A. V. Narlikar, Editor, NOVA Publishers,

SUPERCONDUCTIVITY AND STRUCTURE IN
 $\text{La}_{2-x}\text{M}_x\text{CuO}_4$, M=Ba, Sr, AND (Nd,Sr)

Arnold R. Moodenbaugh
Brookhaven National Laboratory
Upton, NY 11973-5000
moodenba@bnl.gov

1. INTRODUCTION

The identification of charge stripes in $\text{La}_{2-x-y}\text{Nd}_y\text{Sr}_x\text{CuO}_4$ (Nd-214) [1-3] has re-energized research on the original high transition temperature (T_c) superconductor, $\text{La}_{2-x}\text{Ba}_x\text{CuO}_4$ (Ba-214) [4], and related compounds. Early in the study of Ba-214, a low temperature phase transition was associated with changes in electrical properties [5]. An apparent suppression of T_c near Ba $x=0.125$, was initially associated with a first order low temperature phase transformation [6-10]. However, it was later shown that only very near Ba $x=0.125$ was T_c reduced markedly, and that the relationship between crystal structure and T_c is more complicated. This review will describe the low temperature crystal structures and microstructures, as well as the superconducting properties as determined from low field (1-100G) dc magnetometer measurements for Ba-214, Nd-214, and $\text{La}_{2-x}\text{Sr}_x\text{CuO}_4$ (Sr-214). We will also describe some work in the related $\text{La}_{2-x}\text{Ca}_x\text{CuO}_4$ (Ca-214). A basic knowledge of the interactions among superconductivity and low temperature phases will allow us to better understand the significance of the underlying charge stripe phases.

The nominal phase diagram (composition x vs. temperature T) for M=Sr (Ba) is shown in Fig. 1 [after ref. 9]. Above $T=100$ K the systems are similar. The high temperature structure is tetragonal layer perovskite (HTT). With Sr (Ba) substitution for La, the second order transformation temperature to an orthorhombic structure (LTO1) falls below room temperature. For M=Ba, below about $T=70$ K, another phase, having an expanded tetragonal cell (LTT), appears for compositions $x>0.09$. This LTT phase probably extends to $x \approx 0.21$, the LTT/HTT phase boundary. This basic phase diagram as originally described will be essentially unchanged. However, high resolution x-ray diffraction (XRD) and low temperature transmission electron microscopy (TEM) suggest

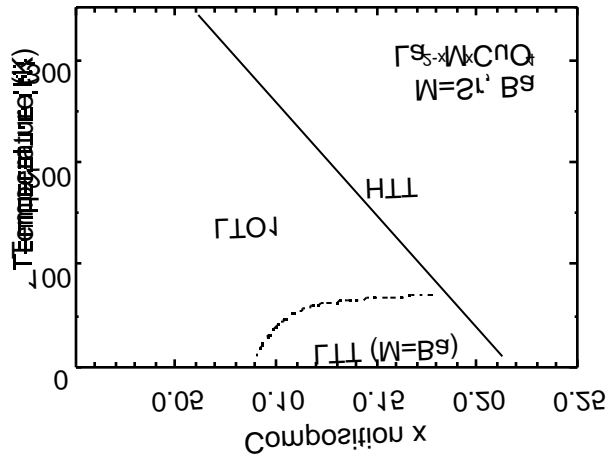


Figure 1. Nominal phase diagram for $\text{La}_{2-x}\text{M}_x\text{CuO}_4$ after Axe, et al. [9]. LTT phase below dashed line is for $M=\text{Ba}$ only. Nominal LTO1 region commonly exhibits $\sim 10\%$ LTT phase below $T \sim 150$ K and $0.05 < x < 0.12$.

of the octahedral edge. This produces a corrugation in the CuO_2 plane. The tilt angle (deviation from vertical) increases as temperature falls, and decreases as a function of x for fixed temperature. The crystal structure has standard space group Cmca , here indexed Bmab to retain c_{ht} . The a_{lto1} and b_{lto1} lattice parameters are rotated 45° from a_{ht} and have magnitude $\sim (\sqrt{2})a_{\text{ht}}$. A schematic diagram of the LTO1-type tilting is shown in Fig. 2a. In the figure the tilt angles are exaggerated and the view is down the c axis. In this LTO1 structure, the microstructure reveals twinning.

The tilting pattern for the LTT structure is shown in Fig. 2b. In this structure the CuO_6 octahedra tilt in the direction of the corners [8,9]. This structure has alternating layers along the c axis (not shown) which tilt 90° away from the illustrated layer. The LTT structure a_{ltt} is similar to the corresponding LTO1 parameters.

An additional distorted layer perovskite phase is commonly encountered in the Rare Earth substituted systems including $\text{La}_{2-x-y}\text{Nd}_y\text{Sr}_x\text{CuO}_4$ [15,16]. The LTO2 phase (pccn space group) can be thought of as a linear superposition of the LTO1 and LTT phases, where the tilts of the CuO_6 octahedra are directed in some intermediate direction [8,9,15].

This paper is organized based on the material systems studied, beginning with section 2 covering $\text{La}_{2-x}\text{Ba}_x\text{CuO}_4$. In each section structures will be described, followed by superconducting properties. A general description of superconducting measurements and properties of polycrystalline high T_c superconductors is included in section 2. A short section 3 provides some information on $\text{La}_{2-x}\text{Ca}_x\text{CuO}_4$. Section 4 covers primarily $\text{La}_{2-x-y}\text{Nd}_y\text{Sr}_x\text{CuO}_4$. Finally there is a short conclusion.

2. $\text{La}_{2-x}\text{Ba}_x\text{CuO}_4$ STRUCTURES AND SUPERCONDUCTIVITY

a more complicated situation. There appear to be wide ranging phase mixtures, especially of minority LTT in nominal LTO1 phase [11].

The phases described above are layer perovskite K_2NiF_4 type [12]. The HTT phase is nominally undistorted with space group I4/mmm , $a_{\text{htt}} \sim 0.38\text{nm}$, $c_{\text{htt}} \sim 1.32\text{nm}$. It has been observed that the local order in this phase is not strictly HTT; the CuO_6 octahedra tilt locally, but without long range order [13-14]. The LTO1 phase occurs when the CuO_6 octahedra tilt away from c_{lto1} in the direction

HTT phase. The high temperature tetragonal (HTT) phase of $\text{La}_{2-x}\text{Ba}_x\text{CuO}_4$ has the $I4/mmm$ space group. The phase is, for $\text{Ba} > 0.21$, stable at the lowest temperatures and is superconducting. This phase, as determined by x-ray and neutron diffraction evidence, is the simplest structure in the system. However, local probes suggest local disorder.

Billinge et al. [17] performed pair distribution function (PDF) analysis of x-ray diffraction data for $\text{Ba } x=0.125$ and 0.15 at temperatures up to 325 K. Their data suggests an LTT-type tilt of the CuO_6 octahedra in the LTO1 phase, and even in the nominal HTT phase. Haskel et al. [18] recently performed x-ray absorption fine structure (XAFS) experiments on oriented $\text{La}_{2-x}\text{Ba}_x\text{CuO}_4$. Their analysis also shows that the CuO_6 octahedral tilt is not changed when going through the LTO1/HTT transformation. Their result is qualitatively consistent with that of Billinge et al. [17], confirming an octahedral tilt in the HTT phase also being consistent with LTT-type tilting in both phases. PDF and XAFS conclusions may be consistent with the HTT diffraction results if the LTT-type tilts are not ordered over large distances. Haskel et al. [18] also looked at the local environment around the Ba species. They found that the local environment is severely distorted relative to the La environment. This suggests an intrinsic local disorder in $\text{La}_{2-x}\text{Ba}_x\text{CuO}_4$ due to the Ba substitution.

Application of high pressure drives the distorted (LTO1 and LTT) phases toward the HTT phase. Early superconductivity measurements suggested that for $\text{Ba } x=0.125$

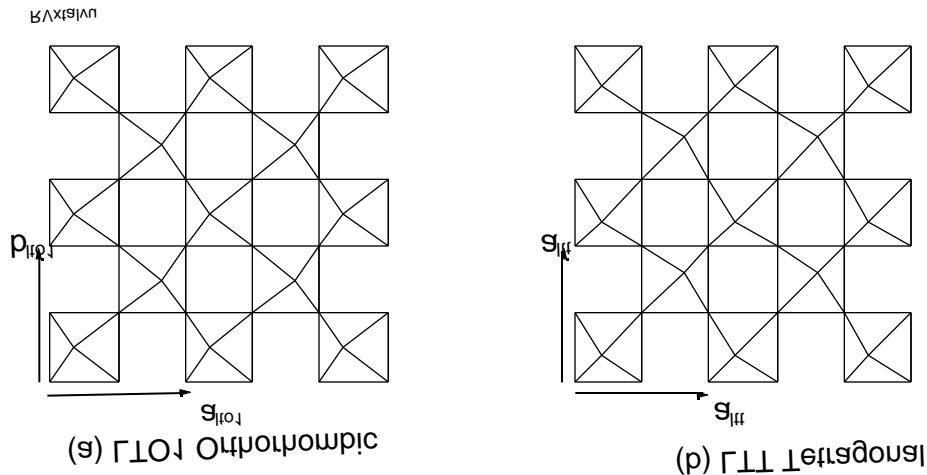


Figure 2. Schematic view down c axis of CuO_6 octahedral layers as seen projected onto the $[001]$ plane illustrating the LTO1 and LTT distortions. Oxygen atoms are at corners of squares, as well as at apices of octahedra. Displacement of apices is exaggerated. (a) In the LTO1 phase the octahedra tilt toward edges, producing a corrugation in the plane. (b) In the LTT phase the octahedra tilt toward the corners.

and pressure $p=20$ kbar, T_c is as high as at neighboring compositions [19]. However, later work [20,21] showed that while T_c increases with pressure, it is still somewhat suppressed near $p=20$ kbar. Because the differences in the subject crystal structures are subtle, and high pressure diffraction experiments may have lower resolution, it is often difficult to determine exactly when the sample becomes HTT under pressure. Crawford [16] has done careful diffraction work which suggests that, for $Ba\ x=0.125$, the HTT phase is not obtained below 20 kbar. Rather, the samples appear to adopt the reduced orthorhombicity characteristic of the LTO2 phase.

LTO1 Phase. The LTO1 phase of $La_{2-x}Ba_xCuO_4$ appears as a low temperature distortion of the HTT phase [8,9]. In diffraction the orthorhombicity increases continuously as temperature drops below the phase transition temperature. It appears that the transition is second order. However, both XAFS [18] and PDF analysis [17] on the HTT phase show that locally, octahedra are tilted at high temperature. A rearrangement of these octahedra across the transition might suggest a first order transition from HTT phase to LTO1 phase.

The local probes (PDF [17] and XAFS [18]) both find that the CuO_6 octahedra are locally tilted in the (110) direction (LTT type) while diffraction suggests a (100) tilt

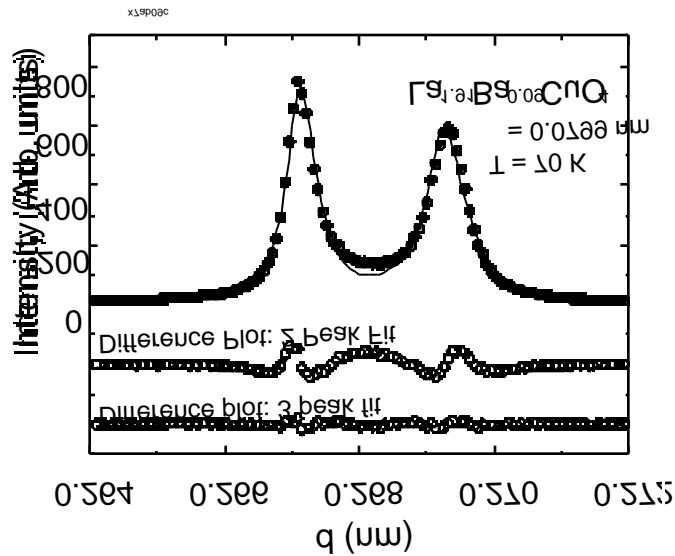


Figure 3. High resolution x-ray diffraction data for the LTO1 phase (200) and (020) peak region for $La_{1.91}Ba_{0.09}CuO_4$ at $T=70$ K. The sample is nominally LTO1. A two peak fit, (solid line) appropriate for the LTO1 phase, shows LTT phase scattering in the corresponding two peak fit difference plot. A three peak fit, incorporating a broad LTT (200) peak, provides an excellent fit to the data.

pattern. In the case of oxygen-reduced $YBa_2Cu_3O_{7-x}$ (1:2:3) a local orthorhombic order due to chain ordering may result in an overall tetragonal structure as determined in diffraction [22]. However, in 1:2:3 there remain microstructural indications of the local orthorhombicity. Transmission electron microscopy (TEM) shows diffuse scattering in diffraction; a “tweed” structure appears in images of the structure [22]. It is puzzling that no such features have been reported in TEM investigations of LTO1 phase $La_{2-x}Ba_xCuO_4$. The only prominent microstructural features are the LTO1 twins.

High resolution x-ray diffraction (HRXRD) has been performed many times on the LTO1 phase of $La_{2-x}Ba_xCuO_4$.

Many of these investigations [8,9,15,23] have concluded that samples are LTO1 phase. In some cases there is evidence of an imperfect fit to the (200), (020) or (400), (040) peak region when two LTO1 peaks are assumed [15]. However, more recent high resolution synchrotron x-ray diffraction studies of $\text{La}_{2-x-y}\text{Nd}_y\text{Sr}_x\text{CuO}_4$ have examined the (200) and (020) peak region through the LTO1/LTT transformation temperature [11]. The peaks here were fit with pseudo-Voigt Lorentzian-Gaussian shapes incorporating peak asymmetry based on the known diffraction geometry of the BNL NSLS X7A beamline [24,25]. It was found that previously unaccounted-for diffraction might reasonably be interpreted as an LTT-type diffraction peak. The LTT peak shape is consistent with a domain size of ~ 50 nm. A similar diffraction scan of nominal LTO1 phase $\text{Ba}_{x=0.09}$ sample at $T=70$ K [26] is shown in Fig. 3. A two peak fit to the data shows excess scattering between the two LTO1 peaks, which corresponds to $\sim 10\%$ of the total diffraction intensity in the segment. A three peak fit, suggesting a minority LTT phase peak between the LTO1 peaks is excellent, as shown by the difference plot at the bottom of the figure. A series of diffraction scans for $\text{Ba}_{x=0.09}$ at a various temperatures are shown in Fig. 4. The parameters obtained from the fits to the data are displayed in Fig. 5. In Fig. 5c, the LTT-type diffraction intensity is present at or above the 10% level from the LTT transition temperature $T_1=40$ K up to 160 K. For this sample the peak FWHM appears to decrease slightly at temperatures below T_1 (Fig. 5b). Lattice constants for both phases are consistent on passing through the transformation (Below $T_1=40$ K, the LTO1 phase peak shapes were fixed to values obtained above T_1 .)

The presence of the LTT-phase minority in nominal LTO1 phase material is a widespread phenomenon also observed in $\text{La}_{2-x}\text{Sr}_x\text{CuO}_4$ [11] and $\text{La}_{2-x-y}\text{Nd}_y\text{Sr}_x\text{CuO}_4$ [26,27]. However there is no observable LTT phase in unsubstituted LTO1 phase La_2CuO_4 down to the 3% level [27]. It might initially be reasonable to relate the LTT minority phase in LTO1 phase material with the LTT-type tilt directions determined from local probes XAFS

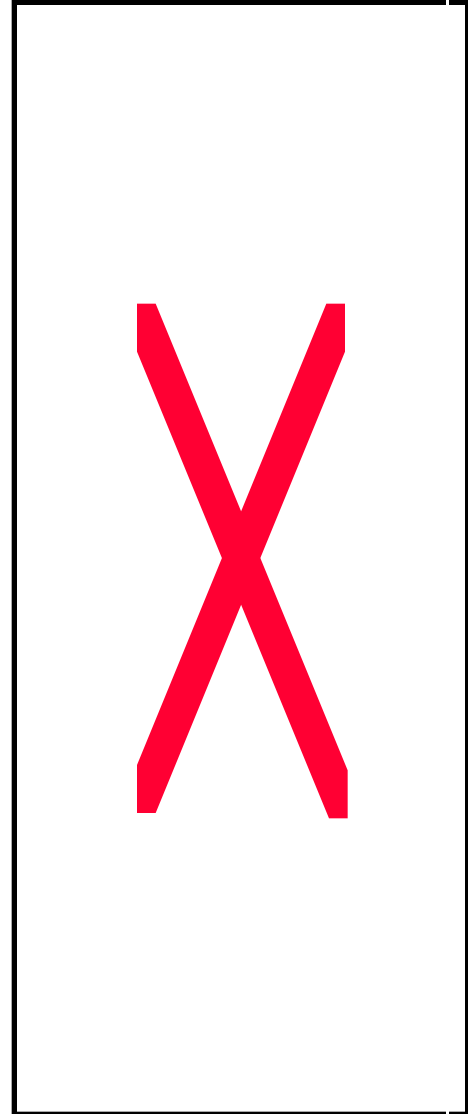


Figure 4. Stack plot of a series of diffraction scans at a series of indicated temperatures for $\text{La}_{1.91}\text{Ba}_{0.09}\text{CuO}_4$. Fits are illustrated by the lines through the data. Above $T=160$ K the fits are for two (LTO1) peaks. Below $T=160$ fits are for three peaks, indicating a phase mixture of LTO1 and LTT phases.

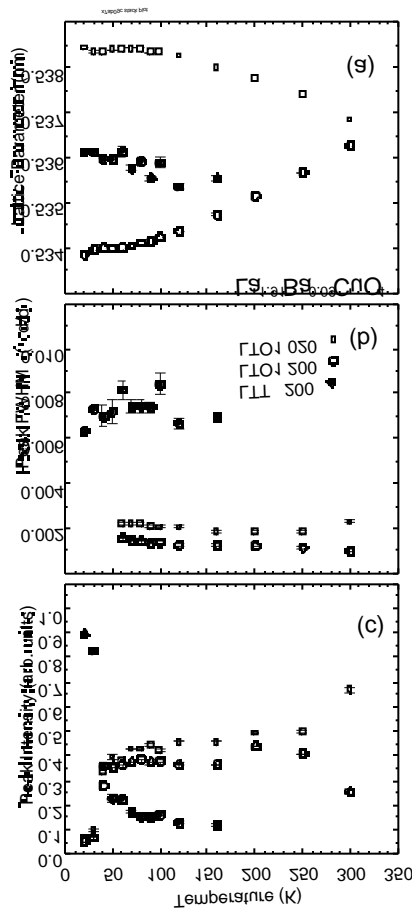


Figure 5. Fitting parameters from the Fig. 4 peak fits for LTO1 and LTT phases. (a) Lattice parameters for LTO1 show the characteristic increase in orthorhombic splitting as temperature is reduced. At lowest temperature fits suggest ~10% LTO1 remaining in LTT phase (for Ba $x > 0.09$ samples appear to be pure LTT at lowest temperatures). (b) Peak full width at half maximum. For this sample the LTO1 and LTT peak widths do not vary greatly through $T_1 = 40$ K. (c) Peak intensities as a function of temperature for the LTO1 (200), (020) and LTT (200) peaks showing the LTO1/LTT transformation temperature to be near $T_1 = 40$ K.

and PDF. However, the local probes find ~100% LTT-type tilting, and there is usually no more than 15% LTT phase in nominal LTO1 phase from HRXRD.

There have been several TEM studies of $\text{La}_{2-x}\text{Ba}_x\text{CuO}_4$ [28-34]. It is often difficult to obtain data on these crystal phases at low temperatures. The low temperature stages are a source of sample drift. Also, the superlattice peaks used to identify the phases [34] are very weak, and often difficult to differentiate from multiple scattering. In general, there are few microstructural features associated with the LTO1 phase, the twin boundaries being prominent. TEM suggest that the <15% minority LTT phase in LTO1 phase $\text{La}_{2-x}\text{Ba}_x\text{CuO}_4$ may be nucleated at the LTO1 twin boundaries [34].

LTT phase. The LTT phase was first observed in $\text{La}_{2-x}\text{Ba}_x\text{CuO}_4$ [5,8,9,35]. This phase has a unit cell, similar to that of the LTO1 phase, in which the a and b axes become equivalent. In diffraction work, (h00) peaks are typically broadened compared to the LTO1 phase (h00) and (0h0) peaks. The transformation from LTO1 to LTT phase appears to be first order, the majority of the transition taking place within a ~10 K interval. We define the LTO1/LTT phase transformation temperature T_1 based on x-ray diffraction data. T_1 is the temperature at which half the diffraction intensity of the (200), (020) diffraction region is found in the LTT phase (200) peak (Fig. 5c) [11].

The approximate phase diagram in Fig. 1 is very similar to the early results of Axe and coworkers [8,9]. In that work, because of the moderate resolution of the diffraction data, it was

not clear how high in x the LTT phase extends at low temperature. Billinge et al., using high resolution x-ray diffraction, [23] showed that the LTT phase extends at least to $x=0.15$. More recently it was observed that, at $x=0.09$ (Fig. 5c), the sample does not transform completely to LTT. Because the transformation is $\sim 90\%$ complete, we can safely say that the Ba content $x=0.09$ is essentially the phase boundary at low temperature between the LTO1 and LTT phases.

In earlier x-ray diffraction experiments, it was often suggested that a portion of LTO1 phase persisted in predominantly LTT material [8,9,23]. In those cases the peaks were often fit with Lorentzian shapes which are probably inappropriate for broadened peaks. Apparent excess intensity in the wings appeared because of the assumption of a Lorentzian peak shape. This extra intensity was interpreted as being due to an LTO1 minority phase. However, we have simulated a (200) peak shape given a domain length of ~ 50 nm [11]. The calculated peak shape is very close to the shape of typical LTT (200) peaks, a pseudo-Voigt 0.7 Gaussian/0.3 Lorentzian. For a Ba $x=0.12$, the observed LTT (200) peaks shapes are consistent with 100% LTT phase at low temperature [27].

Again the apparent simplicity of the diffraction patterns is not wholly consistent with the TEM studies. The early electron microscopy studies by Chen and co-workers [28-30] revealed a complicated microstructure. They observed the LTO1 twin boundaries in the microstructure of the LTT phase material. Between the twin boundaries they observed ~ 30 - 50 nm domains separated by antiphase boundaries. In fact these TEM observations, combined with the observation of the LTT phase nucleating at LTO1 twin boundaries, are the basis for proposing a two step process in the transformation of the LTO1 phase to the LTT phase [11,34] (See Fig. 6). Above T_1 the LTT phase propagates ~ 50 nm from the twin boundaries, but no further. Near T_1 the LTT phase begins to nucleate within the twins. The various domains may not coalesce into a single LTT phase structure because of the antiphase boundaries [29]. Chen et al. also noticed a remaining small and variable orthorhombic distortion in the nominal LTT phase. [28]

Local probes PDF analysis [17] and XAFS [18] both suggest that LTT phase octahedra in $\text{La}_{2-x}\text{Ba}_x\text{CuO}_4$ locally tilt in the [110] set of directions appropriate to the LTT crystal structure. It is ironic that LTT local structure is consistent with the long range structure as determined from diffraction, but shows a complicated microstructure. The LTO1 local structure (octahedra tilting direction) has been determined to be like LTT, implying local disorder, but the microstructure is relatively simple.

Superconductivity. The superconducting properties of $\text{La}_{2-x}\text{Ba}_x\text{CuO}_4$ are affected by the crystal structure at low temperatures, but there is not a direct relationship between crystal structure and superconductivity. The variation of superconducting transition temperature T_c with composition [36] is shown in Fig. 7. When the LTT phase was first discovered, it was linked to a depression of T_c near $x=0.125$ [6,7,37,38]. However, Billinge et al. [23] later demonstrated that a relatively high T_c composition $x=0.15$ retained the LTT phase. Also, samples with composition near $x=0.09$ are nearly completely LTT phase, but the superconducting transition temperature is relatively high at this composition also. The depression of T_c is really associated with the Ba $x=0.125$ (hole content $p=0.125$) composition.

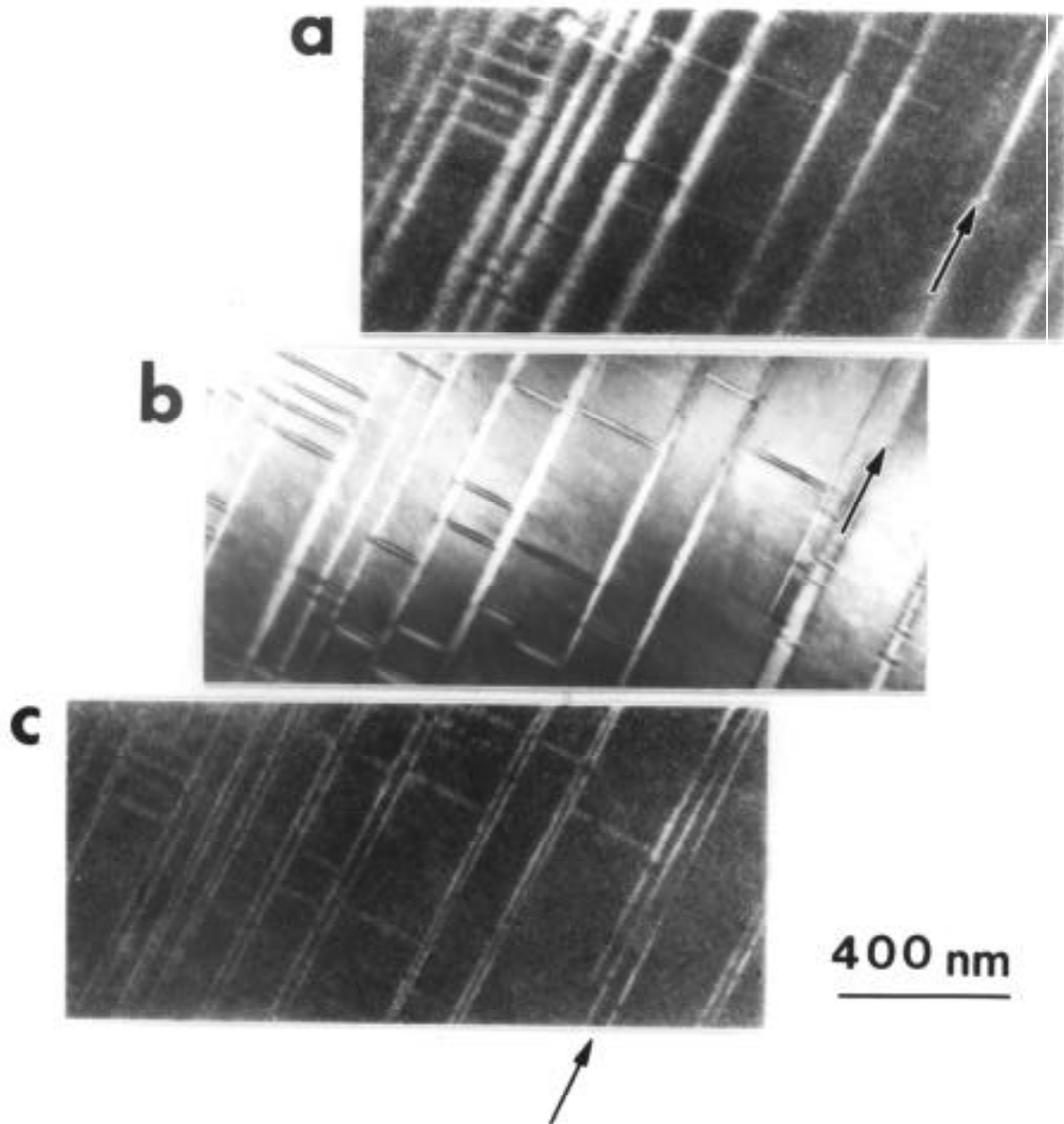


Fig. 6. Electron diffraction contrast observed in $\text{La}_{1.88}\text{Ba}_{0.12}\text{CuO}_4$ at a nominal $T=20$ K. The LTO1 microstructure persists at temperatures at which the LTT phase is predominant in diffraction. (a) A dark field image using the LTO1 superlattice reflection (121) of the $(101)^*$ projection. The twin boundaries are inclined, and only one set of twin domains is illuminated. (b) The bright field image of the same area in the $[001]$ orientation. Image is offset so corresponding twins line up. (c) The dark field image viewed in the same orientation as (b), but using the LTT superlattice (110) reflection. Observe that only the twin boundaries show the bright contrast characteristic of the LTT phase. After Ref. [34].

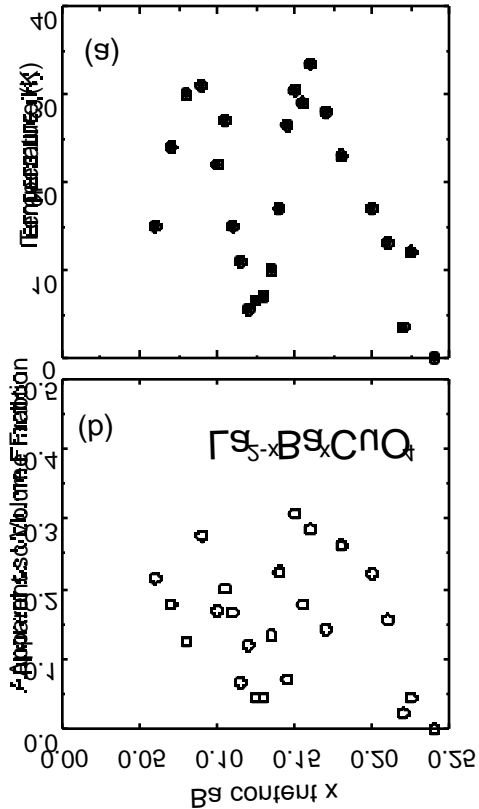


Figure 7. (a) Superconducting transition temperature (onset as determined from zero field cooled low field measurement) as a function of Ba content x . (b) Apparent superconducting volume as a function of Ba x as determined from magnetization measurements made above H_{c1j} (the field at which the grains become decoupled).

always show a significant superconducting transition above 2 K for Ba $x=0.125$. We will describe in detail some of the factors, both intrinsic and extrinsic, that affect the superconducting behavior of polycrystalline samples.

J. R. Clem and Z. Hao [43] calculated the superconducting flux expulsion that might be expected for monolithic samples. Depending on sample shape the apparent superconducting fraction in zero field cooled (ZFC) conditions attains the order of 100%. They showed that for field cooled (FC) samples the apparent superconducting volume (Meissner fraction) could be $<20\%$ of that observed in zero field cooled (ZFC) conditions. The source of the difference is flux pinning, which impedes expulsion of flux in FC conditions.

Additional demonstrations of the requirement for hole content $p=0.125$ come from substitution of species which change the average valence at the La site. Maeno et al. [39] showed that Th (4 valent) substitution for La shifted the minimum in transition temperature to maintain $p=0.125$. Oxygen control studies also suggested that $p=0.125$ has a special significance. First Takayama-Muromachi et al. [40-42], then Moodenbaugh et al. [36], showed that the minimum in T_c follows $p=0.125$ for oxygen reduced samples. As oxygen is removed from the compound, the T_c at the minimum rises compared to fully oxidized samples (but remains low compared with composition adjacent in Ba content x). Takayama-Muromachi et al.[41] showed using low temperature diffraction studies that the oxygen reduced samples remain in the LTT phase, so a change of phase is not the cause of the increase in T_c . The increase in T_c with oxygen removal may be a result of a smearing out of the band structure caused by oxygen disorder [36].

Much has been said about the disappearance of superconductivity near $x=0.125$ and of the relative volume of superconducting material at various compositions. In fact our measurements

In our work we often observe additional problems with low field FC measurements of superconductivity. The sample signal, using a Quantum Design MPMS, behaves normally above the temperature at which flux pinning occurs, the irreversibility temperature [44], showing a superconducting onset. However, at lower temperatures, for many samples, the MPMS interprets the signal as a positive moment; the MPMS signal no longer closely approximates the shape expected from a dipole [27]. Apparently, strong flux pinning within the sample prevents the magnetic flux from approaching equilibrium in these FC measurements.

Another practical problem in measurements of polycrystalline high temperature superconductors is the effect of grain boundaries on the measurements. Clem treated this problem theoretically as an array of superconducting grains connected by more weakly superconducting grain boundaries. This situation is often referred to as the weak-link problem. Clem [45] defined two distinct lower critical fields. H_{c1J} (J for Josephson) represents the critical field for the weak links. In $\text{La}_{2-x}\text{Ba}_x\text{CuO}_4$ and related compounds this field is typically 20 G. Fig. 8 shows magnetization M as a function of applied field H and T_c determined after ZFC. For $H < H_{c1J}$ and temperature well below T_c the apparent superconducting volume from ZFC measurements is ~100%. At some higher field, depending on sample properties, the superconductor exhibits a second critical field, called H_{c1g} (for grains).

Above H_{c1J} the grain boundaries become non-superconducting and the external field can thread through the sample along those grain boundaries. The apparent superconducting volume is significantly reduced (to 10-50% of sample volume). The drastic reduction in volume is due to the penetration depth being the same order of magnitude as the grain size. Because λ is dependent on the crystallographic direction, even the grain shape can affect apparent volume. The value of λ is also known to be composition dependent [46]. Thus the apparent superconducting volume for polycrystalline

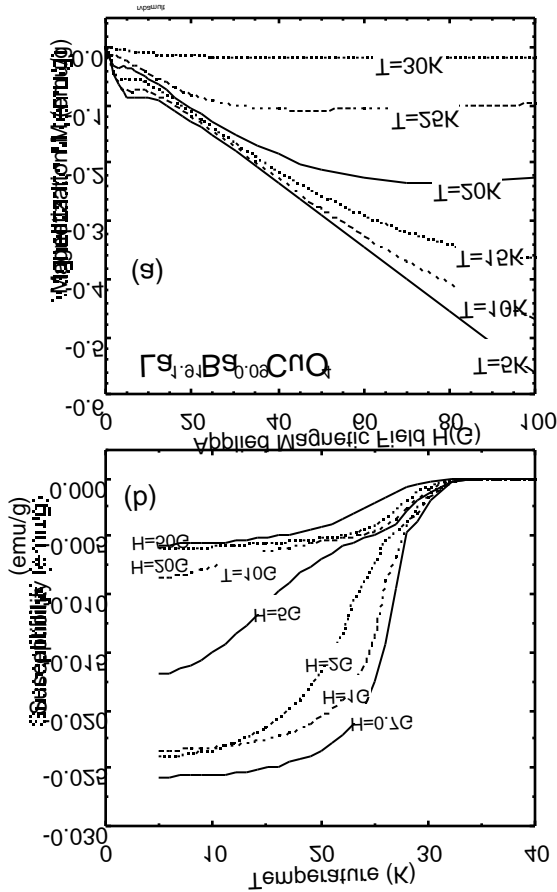


Figure 8. (a) Magnetization as a function of field at a series of temperatures for a sample of $\text{La}_{1.91}\text{Ba}_{0.09}\text{CuO}_4$. Sample is a well sintered polycrystalline pellet. For $T > 20\text{K}$ the full volume superconductivity observed below a few gauss disappears (H_{c1j} tends to 0). (b) Transition curves for the same sample, zero field cooled, at the indicated measuring field. At low fields full volume superconductivity is observed at low temperatures. At higher fields well above H_{c1j} apparent superconducting volume is reduced. Double transitions are especially noticeable for $H = 50\text{G}$. These double transitions are the result of there being two H_{c1} s: H_{c1j} and H_{c1g} .

lation and T_c obtained from a BCS fit to $\chi_{ab}(T)$.

samples is a complicated function of intrinsic properties () as well as of extrinsic properties (microstructure). The earlier investigation by Nagano et al. [46] of $\text{La}_{2-x}\text{Sr}_x\text{CuO}_4$ is a good example of a study based on similar considerations, and we will examine that work in the next section. Those authors opted to powder their samples to a chosen grit. This procedure eliminates the full volume superconductivity observed below H_{c1j} . Consequently the double superconducting transitions encountered for some measuring fields and some sample compositions are avoided. However, an additional complication is that some of the grains will be broken up during the grinding process, while, at the same time, there may be some particles that may still not be single grains.

Fig. 7a shows T_c as a function of composition for $\text{La}_{2-x}\text{Ba}_x\text{CuO}_4$, the value of T_c being taken as the onset temperature determined from low field ZFC measurements [36]. The onset T_c is determined from extrapolating the steepest slope of the magnetization curve to the intersection with zero magnetization. The method gives a reasonably consistent value at low applied field, as long as there is not a double transition due to the applied field being near H_{c1j} (see Fig. 8). Li et al. [47], in a study of Sr-214 single crystals, showed very good correspondence between T_c determined using a similar extrapolation

In Fig. 7b the apparent volume taken from the M/H slope above H_{c1J} after ZFC is plotted. For samples with T_c s below 10K the M/H measurements were taken at $T=2K$. There is considerable scatter, [36,27], but there are also some identifiable trends in the data. The apparent volume fraction of superconductivity increases with Ba content x over a large range of x . This is primarily due to the reduction of penetration depth as holes are doped into the system [46,47]. Much of the scatter is likely due to the variability in sample microstructure. Grain size and shape variations affect the apparent volume fraction as described above. The dependence of χ on temperature also has an effect, especially when the measurement of M/H takes place at $T > 0.5T_c$. There is a noticeable reduction in apparent volume fraction for $x = 0.125$. A similar reduction in χ in the M=Sr system near $x=0.12$ was noted earlier [46,48]. In our data it is not clear whether the reduction in apparent volume fraction of superconductor is due to microstructure or to intrinsic superconducting properties.

The T_c vs. Ba x results should be compared with the low temperature phase diagram shown in Fig. 1. Near the LTO1/LTT phase boundary near $x=0.09$ there is no major change of character of superconductivity. Only for Ba contents near $x=0.12$ is the T_c reduced. Note also that all samples we have prepared near $x=0.12$ have significant superconducting transitions above $T=2K$ [27]; again we emphasize that the Ba $x=0.125$ are superconducting. We have also observed that the choice of starting materials may affect superconducting transition temperatures. In general, T_c s may vary by several degrees, and this variation is reasonably consistent across the superconducting composition range of Ba x .

Another common feature of superconductivity in the Ba-214 system near $x=0.125$ is the existence of a high temperature tail of a few percent of the total signal reaching to $T=30$ K, even for samples with $T_c < 5$ K [6,7]. This suggests there might be an inhomogeneity, perhaps in Ba content, or a low temperature phase mixture of LTT with LTO1 phase. While the diffraction results are consistent with single phase material [26], the low temperature TEM work demonstrates some inhomogeneity at low temperatures [28-30,34].

In summary there is little direct effect of the identity of the stable low temperature phase, whether LTT, LTO1, or HTT, on superconducting properties of $La_{2-x}Ba_xCuO_4$. The compound becomes superconducting near $x=0.06$ in the LTO1 phase (near the insulator/metal boundary) and remains superconducting through the LTT phase composition range, and well into the HTT composition (near $x=0.25$) [6,7]. Within the LTT phase near Ba $x=0.125$, T_c is reduced but samples remain fully or nearly fully superconducting.

3. $La_{2-x}Sr_xCuO_4$

HTT Phase. The $La_{2-x}Sr_xCuO_4$ system was first mapped out by Takagi et al. [12] in connection with an investigation into superconductivity. Except for the absence of an LTT phase, the phase diagram as determined from diffraction studies is similar to

that of $\text{La}_{2-x}\text{Ba}_x\text{CuO}_4$ [46,48,49] (Fig. 1). The HTT phase has been studied using diffraction techniques as well as local probes, XAFS [13] and PDF analysis of diffraction results [50]. TEM studies of the system have also been performed [28-30,33,51]. Radaelli et al. [48] have thoroughly investigated sample preparation techniques. They found that reaction temperatures of 1170°C were necessary to promote single phase samples, especially for $\text{Sr } x > 0.20$. In their opinion, heat treatments between 900°C and $\sim 1100^\circ\text{C}$ are to be avoided because of the partial decomposition of the Sr-214 phase.

In diffraction work the HTT phase in Sr-214 phase appears similar to that observed in Ba-214. But again PDF and XAFS indicate that the relatively simple structure indicated by diffraction analysis may be more complicated on a local level. Haskell et al. [13] showed using XAFS that at low temperature in the nominal HTT phase, for $\text{Sr } x = 0.25$ and 0.30 at low temperature and $x = 0.15$ near room temperature, local tilting of octahedra persists. Bozin et al. [50] performed PDF analysis of diffraction work which, in agreement with the XAFS conclusion, indicated that the octahedra remain tilted in the HTT phase for $x > 0.21$. In this composition range for which the HTT phase is stable at low temperature the PDF analysis could not distinguish the direction of the tilt.

LTO1 Phase. The LTO1 phase in Sr-214 is, from analysis of diffraction data, similar to that of Ba-214. However local probes again distinguish between these two materials. Haskell et al. [13] concluded that their XAFS data for LTO1 phase are consistent only with the (100) expected from crystallographic considerations.

Bozin et al. [50] reported PDF analysis of diffraction data on the LTO1 phase. They found the major tilt direction is (100), in agreement with XAFS and diffraction work for $x = 0$ and $x = 0.05$. For $x > 0.05$ the authors cannot clearly distinguish between tilt directions based on their analysis. However, their work did state that a minority LTT phase at low temperature in LTO1 phase Sr-214 improved their fitting.

The observation of a minority LTT phase in nominal LTO1 phase material is consistent with high resolution x-ray diffraction findings. Moodenbaugh et al. [11] published work on Nd-substituted $\text{La}_{1.88-y}\text{Nd}_y\text{Sr}_{0.12}\text{CuO}_4$ including $y = 0$ (see previous section for details). They found up to 10% LTT minority phase in nominally LTO1 phase Sr-214 for temperatures $< 100\text{ K}$. This work has been extended to other compositions [27] and shows the phase LTO1/LTT phase mixture occurs at low temperatures for $\text{Sr } 0.03 < x < 0.12$. (Above $x = 0.12$ the orthorhombic splitting at low temperature is insufficient to resolve a possible LTT component.)

TEM investigations of the Sr-214 LTO1 phase at low temperatures are not completely consistent. The low temperature TEM investigations are difficult, and the studies described actually utilized different methods. C. H. Chen et al. [28] performed an early TEM study of Sr-214 at several compositions. They found the samples to be homogeneous LTO1 phase, with twins as the major microstructural feature. More recently Horibe et al. [30] reinvestigated the compound ($\text{Sr } x = 0.115$) utilizing dark field imaging of the characteristic LTT (100) peak (forbidden in LTO1 phase). Below $T = 104$ they found scattering characteristic of LTT (or LTO2) phase at twin boundaries and, in addition, at

antiphase domain boundaries within the twins. The conclusions by Horibe et al. appear to be consistent with a minority LTT phase in nominal LTO1 Sr-214 [30].

Superconductivity. Much of the preliminary discussion of superconducting behavior in connection with Ba-214 holds for Sr-214. Takagi et al. [12] first published T_c as a function of temperature in Sr-214. That work showed the essential elements of superconductivity in the high T_c superconductors. For $x > 0.06$, near the insulator-metal boundary T_c rises to a maximum, then falls at higher x . Eventually, superconductivity disappears near $x = 0.25$ although samples remain metallic. Later work showed additional details of T_c variation with composition. Kumagai [37], Takagi et al. [52], Oda et al. [53], and Crawford et al. [54], observed a slight dip in T_c near $x = 0.115$, reminiscent of the more violent variation of T_c near $x = 0.125$ in Ba-214. One report [55] shows a dramatic drop in T_c to below 2 K. Fig. 9 shows T_c and nominal superconducting volume fraction as a function of Sr x [56]. The dip in T_c is apparent near $x = 0.115$, in spite of the sample being nominal (~90%) LTO1 phase at low temperature. There is scatter in the volume fraction of superconductivity, probably introduced by microstructural sample-to-sample variations. There may be a reduction in volume fraction near the same $x = 0.115$ composition [46,48]. No abrupt change in T_c is observed on crossing the LTO1/HTT phase boundary near $x = 0.21$ (compare Fig. 1 with Fig. 9) [46,48].

The details of superconductivity in the Sr-214 system have been studied very thoroughly. Much of the effort, most notably by Nagano et al. [46] and Radaelli et al., [48] was motivated by a report [49] that the HTT phase ($x > 0.21$ at low temperatures) is not superconducting. Nagano used careful preparation and superconductivity measurement techniques to document the superconducting properties of Sr-214. This work relied on powdered samples combined with SEM measurements to determine

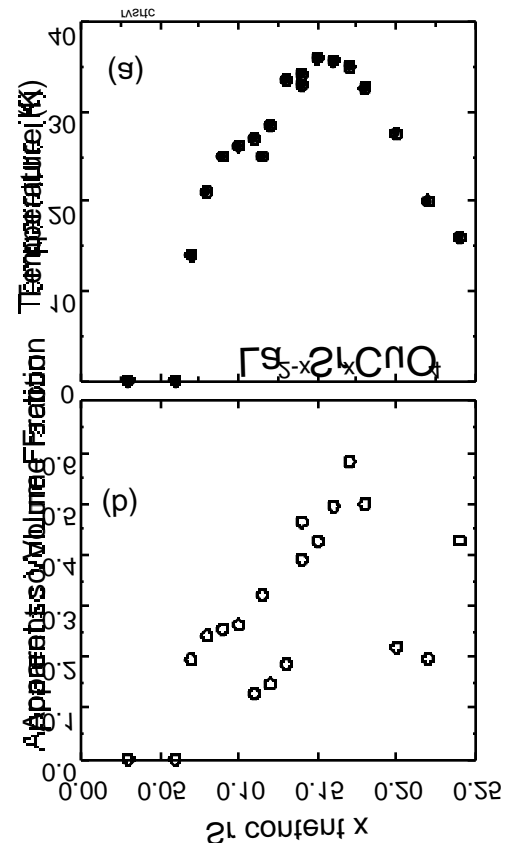


Figure 9. (a) Superconducting transition temperature T_c onset as determined from zero field cooled low field measurements. A slight dip in T_c near $x = 0.115$ is noticeable. (b) The apparent superconducting volumes obtained from ZFC measurements at low temperature of M/H show some scatter. Microstructure of polycrystalline samples, as well as intrinsic superconducting properties, contribute to this quantity.

typical grain sizes along with penetration depth determinations, to provide reliable information on superconducting volume fraction for these samples. The authors concluded that the superconducting properties of Sr-214 vary continuously across the LTO1-HTT phase boundary near $x=0.21$. In addition the authors identified the Sr $x=0.125$ sample as having a relatively low T_c as well as a relatively high λ , resulting in a lower apparent superconducting volume. Radaelli et al. [48] are in agreement with the major results of Nagano et al. [46], Both have similarly low T_c and low apparent volume fractions near $x=0.12$. In Ref. [48] the sample preparation methods and diffraction results were emphasized. Those authors also conclude that superconducting properties are continuous across the LTO1/HTT phase boundary.

Again in the Sr-214 system the superconducting properties are only subtly different across phase boundaries. Across the LTO1/HTT boundary near $x=0.21$ superconducting properties appear continuously varying. Based on the PDF and XAFS observation of local octahedral tilting in the HTT phase, the local environment may be similar on both sides of the boundary. In the nominal Sr-214 LTO1 phase at low temperatures, careful analysis of diffraction reveals the presence of ~10% LTT phase [11]. Apparently linked with the presence of minority LTT phase is a slight reduction in T_c and volume fraction of superconductivity in Sr-214 $x=0.12$. Nagano [46] observed an increase in penetration depth which may account for the reduction in apparent superconducting volume fraction.

4. $\text{La}_{2-x}\text{Ca}_x\text{CuO}_4$

The $\text{La}_{2-x}\text{Ca}_x\text{CuO}_4$ system has been less intensely studied than the $M=\text{Sr}$ and $M=\text{Ba}$ systems. Early work suggested maximum superconducting transition temperatures in the system near 20 K [57-59]. Oh-Ishi et al. [59] estimated a Ca solubility limit $x=0.2$. Fukuoka et al. [60] used high pressure oxygen heat treatment to produce samples with transition temperatures near 35 K. These authors suggested that the solubility limit for samples produced at 1 bar pressure is near $x=0.10$ but, for the high oxygen pressure treated samples, the solubility limit is raised to near $x=0.125$. The authors also allowed an alternative interpretation, the possibility that oxygen deficiency was corrected by the high pressure heat treatments.

Later Moodenbaugh et al. [61] examined the solubility of Ca in La_2CuO_4 in samples prepared at 1 bar oxygen. Using calibrated wavelength-dispersive electron microprobe, they determined the solubility limit to be near $x=0.10$. Dabrowski et al. [62] prepared a series of single phase samples for $x < 0.2$ using high pressure oxygen heat treatments. They found a maximum superconducting transition temperature near 33 K for $x=0.15$. The x dependence of T_c in this $M=\text{Ca}$ system is qualitatively similar to that in the $M=\text{Sr}$ system, with transition temperatures somewhat reduced relative to the $M=\text{Sr}$ system at all compositions [62].

5. $\text{La}_{2-x-y}\text{Nd}_y\text{Sr}_x\text{CuO}_4$ AND OTHER RARE EARTH SUBSTITUTIONS

Structures. Crawford et al. [63] initially investigated partial Rare Earth substitutions for La in $\text{La}_{2-x}\text{Sr}_x\text{CuO}_4$. These compounds, often superconducting, are closely related in structure to the $\text{La}_{2-x}\text{Ba}_x\text{CuO}_4$ superconductors, commonly with LTT phase stable at low temperatures. In addition these materials often have LTO2 crystallographic modifications that were predicted by Axe [8,9], but never clearly observed in the original $\text{La}_{2-x}\text{Ba}_x\text{CuO}_4$ system.

More recently the $\text{La}_{2-x-y}\text{Nd}_y\text{Sr}_x\text{CuO}_4$ system has been utilized as the model system for the study of charge stripes [1-3]. The availability of large single crystals in this system permits the unambiguous observation of charge stripes. Such experiments in $\text{La}_{2-x}\text{Ba}_x\text{CuO}_4$, where stripes are also expected to occur, are not possible because progress in single crystal growth of Ba-214 in that system has proved elusive.

There is general agreement among investigators concerning the low temperature crystallographic phases in $\text{La}_{2-x-y}\text{Nd}_y\text{Sr}_x\text{CuO}_4$. The nominal low temperature phase diagram for the $\text{La}_{2-x-y}\text{Nd}_y\text{Sr}_x\text{CuO}_4$ system is illustrated in Fig. 10, following Buchner and coworkers [64,65]. There

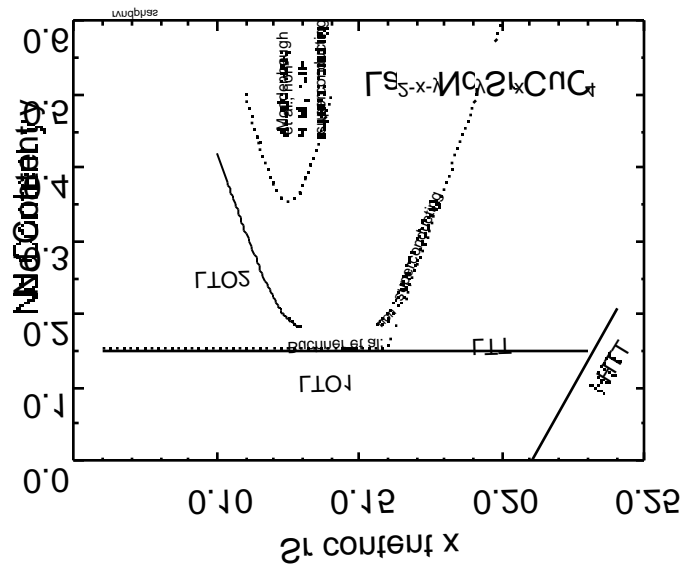


Figure 10. Nominal phase diagram at low temperature for $\text{La}_{2-x-y}\text{Nd}_y\text{Sr}_x\text{CuO}_4$. There is general agreement on the phase diagram. There is disagreement on the extent of superconductivity observed. Illustrated are the superconductor/normal (SN) boundaries as determined by Buchner et al. [64] and by Moodenbaugh et al. [56]. Buchner shows a much more restricted range of superconducting samples. See text for details.

have been noticeable discrepancies in reporting of superconducting properties, with most observers [15,56, 66-68], even those [69] explicitly following the sample preparation methods of Breuer et al. [65], reporting a greater range of superconductivity than Ref. [64].

In work using high resolution x-ray diffraction, the temperature dependence of the structure Sr $x=0.12$, Nd $y=0, 0.01, 0.02$, and 0.04 was reinvestigated [11]. The results are in general agreement with previously published work. However, in the nominal LTO1 phase, there is an $\sim 10\%$ LTT component at temperatures in a range of at least 50 K above the nominal LTO1/LTT (or LTO2) transformation temperature.

Superconductivity. Crawford et al. [15] and Buchner et al. [70] have performed thorough investigations of structure and superconducting properties in this system. Crawford et al. [15] found that superconducting transition temperatures were reduced near the Sr $x=0.12$ composition in LTT samples. Superconducting properties of samples exhibiting LTO2 phase structure are less well understood. Crawford [71] obtained T_c s and determined structure at low temperature for a series of Sr $x=0.12$ samples which suggests that T_c s are intermediate between those observed for LTO1 and LTT phases, and LTT phase samples for a range of compositions are superconducting, but with reduced T_c s. Buchner and coworkers [70,72], however, have consistently reported wide ranges of non-superconducting behavior of LTT phase compositions (see Fig. 10) in a long series of publications [72-82]. In fact, this disagreement prompted a re-evaluation of the system's superconducting properties utilizing polycrystalline samples [56]. In order to determine the superconducting properties in the $\text{La}_{2-x-y}\text{Nd}_y\text{Sr}_x\text{CuO}_4$ system, low field M/H measurements at $H=5\text{K}$ were performed as described in earlier in this review. For this material, magnetization data was obtained for both sintered polycrystalline pellets as well as powders (-400 mesh). The M/H measurements for three sample compositions (all Nd $y=0.40$) are shown in Fig. 11. We will first consider the sintered pellets (dashed lines). For Sr $x=0.10$ the H_{c1j} is either below $H=1\text{G}$ or is non-existent. For low Sr x , the penetration depth may be large, and the sample grains appear to be decoupled at the lowest easily attainable fields $H\sim 1\text{G}$. For Sr $x=0.18$ and $x=0.15$ the sintered pellets show an M/H at low field representing near full volume superconductivity. When H exceeds H_{c1j} ($\sim 5\text{G}$) the magnetization falls. Above H_{c1j} for $x=0.15$ and 18 , the M/H slope is reduced. At some higher field we encounter H_{c1g} , which appears to depend on Sr x . All the powdered samples appear to have decoupled grains at low fields. The M/H slope is reduced somewhat, since grinding the samples unavoidably breaks up some individual grains.

The values of H_{c1g} , the intrinsic critical fields, also shows dependence on x , with H_{c1g} tending to increase from $H \sim 1G$ at $x=0.10$ to near $H=100 G$ at $x=0.18$. In this work we make a rough approximation to H_{c1g} for purposes of a consistent comparison. For powder samples we define H_{c1g} as being the applied field for which the value of M has deviated 10% from the value predicted by a low field fit of M/H . The combination of a relatively low H_{c1g} combined with a noticeable paramagnetic signal from Nd results, at $x=0.10$, results in a positive M for applied fields above $H \sim 100G$ (Fig. 11). In such a situation, a superconductivity measurement would still yield a superconducting transition, but superimposed on a paramagnetic magnetization.

Measurements of samples for a fixed value Sr $x=0.12$ as a function of y are shown in Fig. 12.) These results are ZFC magnetometer measurements at low field on powdered samples. T_c drops quickly for 0.1 y 0.2 but superconductivity is observed for all compositions Sr x 0.3. The T_c s shown in the figure correspond well to results published by Crawford et al. [15]. The approximate H_{c1g} falls swiftly with initial Nd substitution, but plateaus in the range $H=20$ to $30 G$ for $x < 0.3$. The estimated superconducting volume fraction remains similar to that observed for the Nd $y=0$ sample up to Nd $y=0.3$. Only for samples for $y > 0.3$ at Sr $x=0.12$ does superconductivity essentially disappear. These measurements suggest that samples remain superconducting at Sr $x=0.12$ out to a strontium composition Nd $y=0.3$. (Buchner et al. [64] suggest a superconducting/nonsuperconducting boundary near Nd $y=0.18$ at Sr $x=0.12$

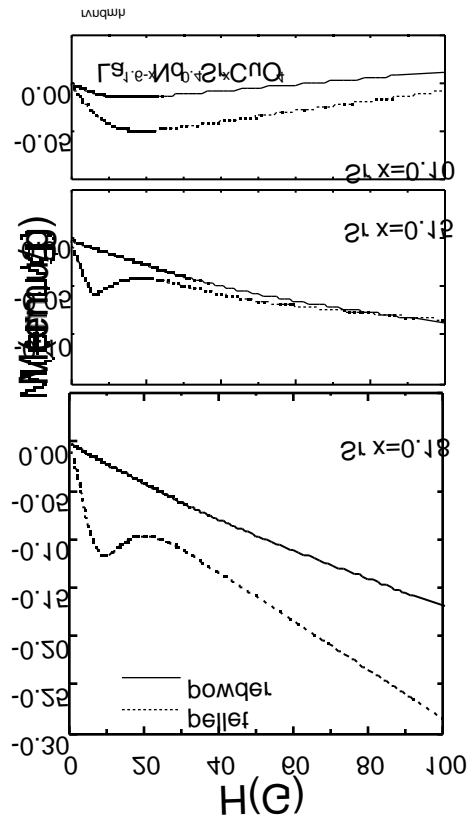


Figure 11. Magnetization as a function of applied magnetic field H for $La_{1.6-x}Nd_{0.4}Sr_xCuO_4$ after cooling in zero field to either $T=2 K$ (Sr $x=0.10,0.15$) or $T=5 K$ (Sr $x=0.18$). Dotted lines represent M for sintered polycrystalline pellets while solid line traces M for powdered samples.

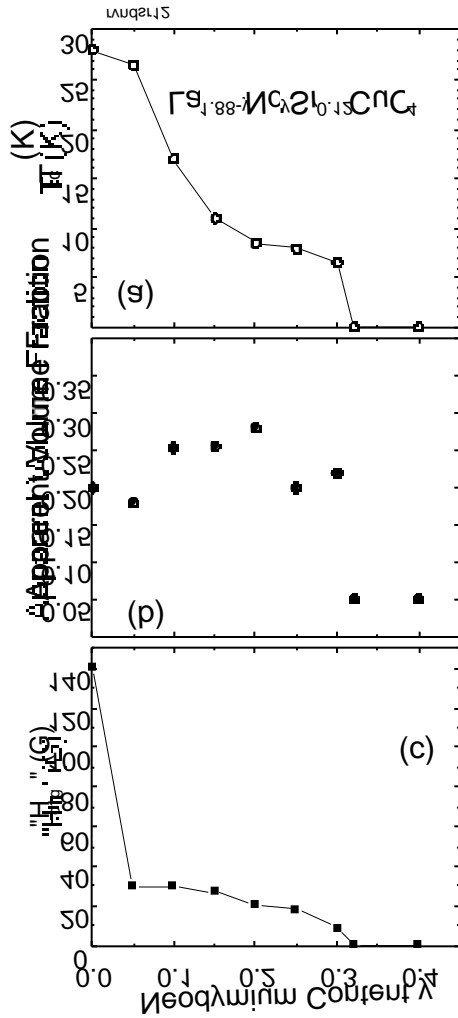


Figure 12. Superconducting properties for a series of samples $\text{La}_{1.88-y}\text{Nd}_y\text{Sr}_{0.12}\text{CuO}_4$. Top panel shows T_c as a function of Nd content x . Center panel shows apparent volume fraction of superconductor as determined for powdered samples from slope M/H at low field H . Bottom panel indicates approximate H_{c1g} determined as described in the text.

magnetic contribution of Nd, those authors determined that the sample is a good bulk superconductor. In our view the neutron scattering measurements [1-3], considered with superconductivity measurements, provide strong evidence for the coexistence of static charge stripes and superconductivity in the $\text{La}_{2-x-y}\text{Nd}_y\text{Sr}_x\text{CuO}_4$ system. [69]

A close examination of superconductivity in the crystals used in the stripe phase studies [1,2,83] revealed these samples to be superconducting [3,84]. Crystals of composition Nd $y=0.4$, Sr $x=0.12, 0.15$, and 0.20 all exhibit charge stripe order as well as superconducting transitions with $T_{cs} = 3.5, 11$, and 15 K respectively. The interpretation of superconductivity measurements of single crystals can be misleading. ZFC estimates of superconductivity can overestimate superconducting volume because of demagnetization effects. In addition a superconducting shell can shield a nonsuperconducting or partly nonsuperconducting interior, also leading to an overestimate of superconducting volume. These ZFC measurements suggest a full volume superconductor (calculations for all three compositions lead to $>100\%$ superconducting volume fraction for all three compositions). However the relative volume for the $x=0.12$ sample is reduced relative to the $x=0.15$ and $x=0.20$ crystals.

Ostenson et al. [84] studied one of these crystals, Nd $y=0.4$ and Sr $x=0.15$, using high field techniques to probe the volume of the sample in the reversible regime. They chose the Sr $x=0.15$ sample since its higher T_c permits more convenient continuous operation above $T=4.5$ K with the sample in the superconducting state. After making careful correction for the

Nachumi et al. [85] performed muon spin relaxation on crystals with $\text{Nd } y=0.4$, $\text{Sr } x=0.15$ and $x=0.20$. They demonstrated, by pulverizing a portion of the $x=0.15$ crystal, that the entire sample supports magnetic order. The observation supports the conclusion that superconductivity coexists with stripe order.

6. DISCUSSION

The Ba-214, Sr-214, and (Nd,Sr)-214 systems have many similarities. The availability of single crystals in the (Nd,Sr)- system allows charge stripes to be studied in detail in this model system. It is believed that static charge stripes also exist in the Ba-214 system, but the lack of single crystals inhibits the investigation. In the Sr-214 system, phenomena believed to be related to charge stripe order have also been observed. [55,86-89]

The overall picture of superconductivity in these systems is, in our opinion, one of gradual variation across phase boundaries. Often local probes suggest that these systems have similar local structure, in spite of the differences in average structures determined by x-ray and neutron diffraction. The model of a superconducting/nonsuperconducting boundary put forward by Buchner et al. [64] seems, at least for typical samples, to be inappropriate. The FC magnetic measurements underlying those conclusions are insufficiently described to compare those results directly with other data. Most investigators, even those following similar sample preparation techniques [69], obtain higher superconducting transition temperatures similar to those reported by other investigators. The discrepancies are probably too great to attribute fully to differences in measurement methods or interpretation; there are very likely differences in sample properties.

In the measurement of superconducting transitions, it might be expected to observe two distinct transitions in two-phase samples, and an apparent two-phase behavior is often observed in polycrystalline samples. However, the apparent two phase behavior is often due to the effects of two critical fields, H_{c1j} for grain boundaries, and H_{c1g} for grains [45]. Measurements of T_c performed at a low applied field H near H_{c1j} will result in an apparent double transition in good single phase material (See Fig. 8).

There is no solid evidence for true two phase behavior in superconducting properties, either superconducting/non-superconducting (SN) or superconducting/superconducting (SS). SN might be expected in phases with pinned charge stripes. There is some suggestion of a reduced superconducting volume in some experiments [46,48], but no clear evidence for the behavior.

SS behavior might be expected in the LTO1/LTT phase mixtures observed at low temperatures. There is no clear evidence for this behavior, either. Commonly, for $M=\text{Sr}$ at low temperatures, the LTO1 phase predominates with ~ 50 nm LTT inclusions or precipitates for $\text{Sr } 0.03 \leq x \leq 0.12$. The apparent superconducting volume seems to be reduced only near $\text{Sr } x=0.12$. The LTT phase predominates at low temperatures, in the $M=\text{Ba}$ system for $\text{Ba } x > 0.09$. However, there are low temperature microstructures and, perhaps, slight local orthorhombicity [28]. Samples appear superconducting at all

compositions, with apparent volume fraction reduced near Ba $x=0.12$ [36]. There may be some indication of an SS phase mixture for Ba $x=0.125$, with the gradual superconducting onset near $T=30$ K and the bulk $T_c < 5$ K.

It appears that charge stripes are more readily pinned in the LTT structure. The charge stripes may be pinned due to a local structural feature. However, when a mixture of LTT and LTO1 phases exists, the electrical and magnetic properties of the entire system, both LTT and LTO1 phases, seem to be affected equally. There is little or no good evidence for a true two phase behavior in observed superconducting properties.

ACKNOWLEDGEMENTS

Research at Brookhaven National Lab is supported by the U. S. Department of Energy, Office of Basic Energy Sciences, Division of Materials Science, under Contract DE-AC02-98CH10886. The National Synchrotron Light Source at Brookhaven is also supported by the Division of Chemical Sciences.

In 1987 John Axe proposed an investigation into the low temperature structural behavior of Ba-214 based on his reading of Ref. [5]. Dave Cox, John Axe, Mas Suenaga, Youwen Xu, Yimei Zhu, John Tranquada, and many other Brookhaven colleagues have studied these high temperature superconductors, participating in collaborations involving many institutions.

REFERENCES

- [1] J. M. Tranquada, B. J. Sternlieb, J. D. Axe, Y. Nakamura, and S. Uchida, *Nature* **375** (1995) 561.
- [2] J. M. Tranquada, J. D. Axe, N. Ichikawa, Y. Nakamura, S. Uchida, and B. Nachumi, *Phys. Rev. B* **54** (1996) 7489.
- [3] J. M. Tranquada, J. D. Axe, N. Ichikawa, A. R. Moodenbaugh, Y. Nakamura, and S. Uchida, *Phys. Rev. Lett.* **78** (1997) 338.
- [4] J. G. Bednorz and K. A. Muller, *Z. Phys. B* **64** (1986) 189.
- [5] D. McK. Paul, G. Balakrishnan, N. R. Bernhoeft, W. I. F. David, and W. T. A. Harrison, *Phys. Rev. Lett* **58** (1987) 1976.
- [6] A. R. Moodenbaugh, Y. Xu, and M. Suenaga, p. 427 in: M. B. Brodsky, et al. (Eds.), High Temperature Superconductors, Mater. Res. Soc. Symp. Proc V. 99 (MRS, Pittsburgh, 1988).
- [7] A. R. Moodenbaugh, Youwen Xu, M. Suenaga, T. J. Folkerts, and R. N. Shelton, *Phys. Rev. B* **38** (1988) 4596.
- [8] J. D. Axe, D. E. Cox, K. Mohanty, H. Moudden, A. R. Moodenbaugh, Youwen Xu, and T. R. Thurston, *IBM J. Res. Dev.* **33** (1989) 382.
- [9] J. D. Axe, A. H. Moudden, D. Hohlwein, D. E. Cox, K. M. Mohanty, A. R. Moodenbaugh, and Youwen Xu, *Phys Rev. Lett.* **62** (1989) 2751.
- [10] D. E. Cox, P. Zolliker, J. D. Axe, A. H. Moudden, A. R. Moodenbaugh, and Y. Xu, p. 141 in: J. D. Jorgensen, et al. (Eds.), High Temperature Superconductors:

Relationships Between Properties, Structure, and Solid State Chemistry, Mater. Res. Soc. Symp. Proc. V. 156 (MRS, Pittsburgh, 1989).

- [11] A. R. Moodenbaugh, L. Wu, Y. Zhu, L. H. Lewis and D. E. Cox, Phys. Rev. B **58** (1998) 9549.
- [12] H. Takagi, S. Uchida, K. Kitazawa, and S. Tanaka, Jpn. J. Appl. Phys. **26** (1987) L123.
- [13] D. Haskel, E. A. Stern, D. G. Hinks, A. W. Mitchell, J. D. Jorgensen, and J. I. Budnick, Phys. Rev. Lett **76** (1996) 439.
- [14] E. S. Bozin and S. J. L. Billinge, Physica B **241-243** (1998) 795.
- [15] M. K. Crawford, R. L. Harlow, E. M. McCarron, W. E. Farneth, J. D. Axe, H. Chou, and Q. Huang, Phys. Rev. B **44** (1991) 7749.
- [16] M. K. Crawford, R. L. Harlow, E. M. McCarron, S. W. Tozer, Q. Huang, D. E. Cox, and Q. Zhu, p. 281 in: E. Kaldis et al. (Eds.), High T_c Superconductivity 1996: Ten Years After the Discovery, (Kluwer, Netherlands, 1997).
- [17] S. J. L. Billinge, G. H. Kwei, and H. Takagi, Phys. Rev. Lett. **72** (1994) 2282.
- [18] Daniel Haskel, E. A. Stern, F. Dogan, and A. R. Moodenbaugh, Phys. Rev. B., in press.
- [19] N. Yamada, M. Oda, M. Ido, Y. Okajima, and K. Yamaya, Solid State Commun. **70** (1989) 1151.
- [20] N. Yamada and M. Ido. Physica C **203** (1992) 240.
- [21] W. J. Liverman , J. G. Huber, A. R. Moodenbaugh, and Youwen Xu, Phys. Rev. B **45** (1992) 4897.
- [22] Youwen Xu, M. Suenaga, J. Tafto, R. L. Sabatini, A. R. Moodenbaugh, and P. Zolliker, Phys. Rev. B **39** (1989) 6667.
- [23] S. J. L. Billinge, G. H. Kwei, A. C. Lawson, J. D. Thompson, and H. Takagi, Phys. Rev. Lett **71** (1993) 1903.
- [24] B. van Laar and W. B. Yelon, J. Appl. Cryst. **17** (1984) 47.
- [25] L. W. Finger, D. E. Cox, and A. P. Jephcoat, J. Appl. Cryst. **27** (1992) 892.
- [26] A. R. Moodenbaugh and D. E. Cox, submitted to Physica C.
- [27] A. R. Moodenbaugh, Unpublished.
- [28] C. H. Chen, S.-W. Cheong, D. J. Werder, A. S. Cooper, and L. W. Rupp, Jr., Physica C **175** (1991) 301.
- [29] C. H. Chen, D. J. Werder, S.-W. Cheong, and H. Takagi, Physica C **183** (1991) 121.
- [30] Y. Horibe, Y. Inoue, and Y. Koyama, Physica C **282-287** (1997) 1071.
- [31] C. H. Chen, S.-W. Cheong, D. J. Werder, and H. Takagi, Physica C **206** (1993) 183.
- [32] Y. Inoue, Y. Wakabayashi, K. Ito, and Y. Koyama, Physica C **235-240** (1994) 835.
- [33] Y. Koyama, Y. Wakabayashi, K. Ito, and Y. Inoue, Phys. Rev. B **51** (1995) 9045.
- [34] Yimei Zhu, A. R. Moodenbaugh, Z. X. Cai, J. Tafto, M. Suenaga, and D. O. Welch, Phys. Rev. Lett. **73** (1994) 3026.
- [35] T. Suzuki and T. Fujita, Physica C **159** (1989) 111.

- [36] A. R. Moodenbaugh, U. Wildgruber, Y. L. Wang, and Youwen Xu, *Physica C* **245** (1995) 347.
- [37] K. Kumagai, Y. Nakamura, I. Watanabe, Y. Nakamichi, and H. Nakajima, *J. Mag. Mag. Mater.* **76-77** (1988) 601.
- [38] M. Sera, Y. Ando, S. Kondoh, K. Fukuda, M. Sato, I. Watanabe, S. Nakashima, and Y. Kumagai, *Solid State Commun.* **69** (1989) 851.
- [39] Y. Maeno, N. Kakehi, M. Kato, and T. Fujita, *Phys. Rev. B.* **44** (1991) 7753.
- [40] E. Takayama-Muromachi, *Physica C* **185-189** (1991) 833.
- [41] E. Takayama-Muromachi, F. Izumi, and T. Kamiyama, *Physica C* **215** (1993) 329.
- [42] E. Takayama-Muromachi and D. E. Rice, *Physica C* **177** (1991) 195.
- [43] J. R. Clem and Z. Hao, *Phys. Rev. B* **48** (1993) 13774.
- [44] Qiang Li, M. Suenaga, T. Kimura, and K. Kishio, *Phys. Rev. B* **47** (1993) 11384.
- [45] J. R. Clem, *Physica C* **153-155** (1988) 50.
- [46] T. Nagano, Y. Tomioka, Y. Nakayama, K. Kishio, and K. Kitazawa, *Phys. Rev. B* **48** (1993) 9689.
- [47] Qiang Li, M. Suenaga, T. Kimura, and K. Kishio, *Phys. Rev. B* **47** (1993) 2854.
- [48] P. G. Radaelli, D. G. Hinks, A. W. Mitchell, B. A. Hunter, J. L. Wagner, B. Dabrowski, K. G. Vandervoort, H. K. Viswanathan, and J. D. Jorgensen, *Phys. Rev. B* **49** (1994) 4163.
- [49] H. Takagi, R. J. Cava, M. Marezio, B. Batlogg, J. J. Krajewski, W. F. Peck, Jr., P. Bordet, and D. E. Cox, *Phys. Rev. Lett.* **68** (1992) 3777.
- [50] E. S. Bozin, S. J. L. Billinge, G. H. Kwei, and H. Takagi, *Phys. Rev. B* **59** (1999) 4445.
- [51] Y. Koyama, Y. Wakabayashi, and Y. Inoue, *Physica C* **235-240** (1994) 833.
- [52] H. Takagi, T. Ido, S. Ishibashi, M. Uota, S. Uchida, and Y. Tokura, *Phys. Rev. B* **40** (1989) 2254.
- [53] M. Oda, T. Nakano, Y. Kamada, and M. Ido, *Physica C* **183** (1991) 234.
- [54] M. K. Crawford, W. E. Farneth, E. M. McCarron III, R. L. Harlow, and A. H. Moudden, *Science* **250** (1990) 1390.
- [55] K. Kumagai, K. Kawano, I. Watanabe, K. Nishiyama, and K. Nagamine, *J. Superconductivity* **7** (1994) 63.
- [56] A. R. Moodenbaugh, L. H. Lewis, and S. Soman, *Physica C* **290** (1997) 98.
- [57] K. Kishio, K. Kitazawa, S. Kanbe, I. Yasuda, N. Sugii, H. Takagi, S. Uchida, K. Fueki, and S. Tanaka, *Chem Lett.* (1987) 429.
- [58] K. Kishio, K. Kitazawa, N. Sugii, S. Kanbe, K. Fueki, H. Takagi, and S. Tanaka, *Chem Lett.* (1987) 635.
- [59] K. Oh-ishi, M. Kikuchi, Y. Syono, N. Kobayashi, T. Sasaoka, T. Matsushira, Y. Muto, and H. Yamauchi, *Jpn. J. Appl. Phys.* **27** (1988) L1449.
- [60] M. Fukuoka, Y. Nakayama, Y. Tomioka, K. Kishio, and K. Kitazawa, *Physica C* **190** (1991) 91.
- [61] A. R. Moodenbaugh, R. L. Sabatini, Youwen Xu, John Ochab, and J. G. Huber, *Physica C* **198** (1992) 103.

- [62] B. Dabrowski, Z. Wang, J. D. Jorgensen, R. L. Hitterman, J. L. Wagner, B. A. Hunter, and D. G. Hinks, *Physica C* **217** (1993) 455.
- [63] M. K. Crawford, M. N. Kunchur, W. E. Farneth, E. M. McCarron III, and S. J. Poon, *Phys. Rev. B* **41** (1990) 282.
- [64] B. Buchner, M. Breuer, A. Freimuth, and A. Kampf, *Phys. Rev. Lett.* **73** (1994) 1841.
- [65] M. Breuer, B. Buchner, R. Muller, M. Cramm, O. Maldonado, A. Freimuth, B. Roden, R. Borowski, B. Heymer, and D. Wohlleben, *Physica C* **208** (1993) 217.
- [66] M. Maki, M. Sera, M. Hiroi, and N. Kobayashi, *Phys. Rev. B* **56** (1996) 11324.
- [67] M. K. Crawford, R. L. Harlow, E. M. McCarron, W. E. Farneth, N. Herron, H. Chou, and D. E. Cox, *Phys. Rev. B* **47** (1993) 11623.
- [68] D. A. Wright, R. A. Fisher, N. E. Phillips, M. K. Crawford, and E. M. McCarron III, *Physica B* **194-196** (1994) 469.
- [69] M. Singer, A. W. Hunt, A. F. Cederstrom, and T. Imai, *Phys. Rev. B* **60** (1999) 15345.
- [70] B. Buchner, M. Braden, M. Cramm, W. Schlabitz, W. Hoffels, W. Braunisch, R. Muller, G. Heger, and D. Wohlleben, *Physica C* **185-189** (1991) 903.
- [71] M. K. Crawford, W. E. Farneth, R. L. Harlow, E. M. McCarron, R. Miao, H. Chou, and Q. Huang, p. 531 in: Y. Bar-Yam, T. Egami, J. Mustre-deLeon, and A. R. Bishop, Eds, Lattice Effects in High-T_c Superconductors (World Scientific, Singapore, 1992).
- [72] B. Buchner, M. Breuer, M. Cramm, A. Freimuth, H. Micklitz, W. Schlabitz, and A. P. Kampf, *J. Low Temp. Phys.* **95** (1994) 285.
- [73] B. Buchner, M. Cramm, M. Braden, W. Braunisch, O. Hoffels, W. Schnelle, J. Harnischmacher, R. Borowski, A. Greutz, B. Heymer, C. Hohn, R. Muller, O. Maldonado, A. Freimuth, W. Schlabitz, G. Heger, D. J. Khomski, and D. Wohlleben, p. 349 in: R. Kossowsky et al. (Eds.), Physics and Materials Science of High Temperature Superconductors, II (Kluwer, Dordrecht, 1992).
- [74] B. Buchner, M. Breuer, W. Schlabitz, A. Viack, W. Schafer, a. Freimuth, and A. P. Kampf, *Physica C* **235-240** (1994) 281.
- [75] T. Niemoller, B. Buchner, M. Cramm, C. Huhnt, L. Troger, and M. Tischer, *Physica C* **299** (1998) 191.
- [76] M. Braden, O. Hoffels, W. Schnelle, B. Buchner, G. Heger, B. Hennion, I. Tanaka, and H. Kojima, *Phys. Rev. B* **47** (1993) 12288.
- [77] O. Baberski, A. Lang, O. Maldonado, M. Hucker, B. Buchner, and A. Freimuth, *Europhys. Lett.* **44** (1998) 335.
- [78] B. Buchner, M. Cramm, M. Braden, W. Braunisch, O. Hoffels, W. Schnelle, R. Muller, A. Freimuth, W. Schlabitz, G. Heger, D. I. Khomskii, and D. Wohlleben, *Europhys. Lett.* **21** (1993) 953.
- [79] M. Cramm, B. Buchner, A. Fiack, E. Holland-Moritz, R. Muller, W. Schlabitz, M. Braden, and D. Hohlwein, *Physica C* **235-240** (1994) 855.

- [80] V. Kataev, B. Rameev, B. Buchner, M. Hucker, and R. Borowski, *Phys. Rev. B* **55** (1997) R3394.
- [81] M. Breuer, W. Schafer, N. Knauf, B. Roden, W. Schlabitz, B. Buchner, M. Cramm, and R. Muller, *Physica C* **235-240** (1994) 345.
- [82] B. Buchner, A. Freimuth, M. Breuer, A. Lang, H. Micklitz, and A. P. Kampf, *Physica C* **235-240** (1994) 1227.
- [83] Y. Nakamura and S. Uchida, *Phys. Rev. B* **46** (1992) 5841.
- [84] J. E. Ostenson, S. Bud'ko, M. Breitwisch, D. K. Finnemore, N. Ichikawa, and S. Uchida, *Phys. Rev. B* **56** (1997) 2820.
- [85] B. Nachumi, Y. Fudamoto, A. Keren, K. M. Kojima, M. Larkin, G. M. Luke, J. Merrin, O. Tchernyshyov, Y. J. Uemura, N. Ichikawa, M. Goto, H. Takagi, S. Uchida, M. K. Crawford, E. M. McCarron, D. E. MacLaughlin, R. H. Heffner, *Phys. Rev. B* **58** (1998) 8760.
- [86] T. Suzuki, Y. Oshima, K. Chiba, T. Fukase, T. Goto, H. Kimura, and K. Yamada, *Phys. Rev. B* **60** (1999) 10500.
- [87] H. Matsushita, H. Kimura, M. Fujita, K. Yamada, K. Hirota, and Y. Endoh, *J. Phys. Chem Solids* **60** (1999) 1071.
- [88] S. Ohsugi, Y. Kitaoka, H. Yamanaka, K. Ishida, and K. Asayama, *J. Phys. Soc. Jpn.* **63** (1994) 2057.
- [89] T. Suzuki, T. Goto, K. Chiba, T. Shinoda, T. Fukase, H. Kimura, K. Yamada, M. Ohashi, and Y. Yamaguchi, *Phys. Rev. B* **57** (1998) R3229.